

Bootstrapping mesons at large N

Jan Albert



2203.11950, 2307.01246 w/ L. Rastelli

2312.15013 + wip w/ J. Henriksson, L. Rastelli, A. Vichi

Strings 2024 



Stony Brook University

Large N QCD

We consider 4-dimensional QCD with N_f **massless** quarks in 't Hooft's **large N** limit. At leading order in $1/N$, the theory decomposes into three **decoupled** sectors of **stable** asymptotic states:

- **Mesons**
 $q\bar{q}$

- Baryons
 $\epsilon_{ij\dots k} q^i q^j \dots q^k$

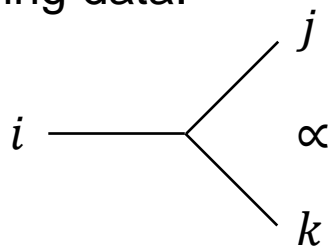
- Glueballs
 $\text{Tr}(F^\#)$

Large N QCD

We consider 4-dimensional QCD with N_f **massless** quarks in 't Hooft's **large N** limit. At leading order in $1/N$, the theory decomposes into three **decoupled** sectors of **stable** asymptotic states:

- **Mesons**
 $q\bar{q}$
- **Baryons**
 $\epsilon_{ij\dots k} q^i q^j \dots q^k$
- **Glueballs**
 $\text{Tr}(F^\#)$

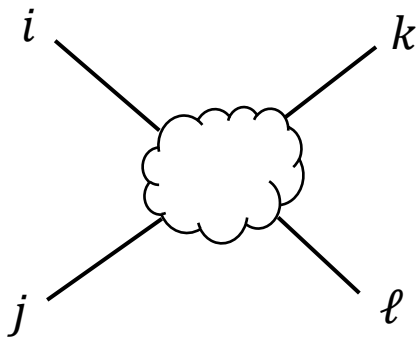
We will focus on the meson sector. The theory then consists of an infinite collection of **weakly coupled** mesons. We parametrize it with the following data:

$$\{(m_i^2, J_i), \lambda_{ijk}, \lambda_{ijkl}, \dots\}$$

$$\propto \lambda_{ijk} \sim \frac{1}{\sqrt{N}}$$

We will proceed to place **bounds** on these data.

Bootstrap philosophy

These data parametrize a space of putative “large N confining gauge theories”. We will carve out allowed regions in it by requiring consistency of meson S -matrices.



S-matrix Bootstrap

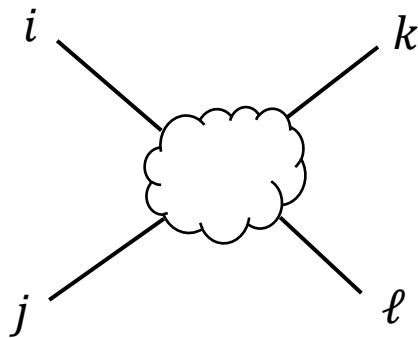
- Unitarity
- Regge boundedness
- Crossing symmetry
- ...

[Martin 1969, Pham & Truong 1985, Ananthanarayan et al.1995, ...]

[Caron-Huot, Van Duong 2021, Tolley, Wang, Zhou 2021, Arkani-Hamed, Huang, Huang 2020]

Bootstrap philosophy

These data parametrize a space of putative “large N confining gauge theories”. We will carve out allowed regions in it by requiring consistency of meson S -matrices.



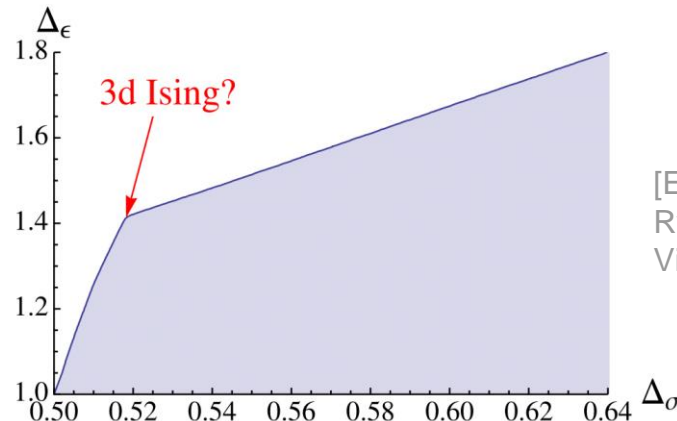
S-matrix Bootstrap

- Unitarity
- Regge boundedness
- Crossing symmetry
- ...

[Martin 1969, Pham & Truong 1985, Ananthanarayan et al.1995, ...]

[Caron-Huot, Van Duong 2021, Tolley, Wang, Zhou 2021, Arkani-Hamed, Huang, Huang 2020]

The goal is to choose the right set of assumptions that will corner large N QCD, much like the Ising model in the CFT bootstrap.



[El-Showk, Paulos, Poland, Rychkov, Simmons-Duffin, Vichi 2012]

Pion scattering

We start by scattering the lowest mesons in the spectrum, the pions π^a , which are Goldstone bosons for

$$U(N_f)_L \times U(N_f)_R \rightarrow U(N_f)_{\text{diag}}.$$

[Coleman, Witten 1980]

Pion scattering

We start by scattering the lowest mesons in the spectrum, the pions π^a , which are Goldstone bosons for

$$U(N_f)_L \times U(N_f)_R \rightarrow U(N_f)_{\text{diag}}. \quad [\text{Coleman, Witten 1980}]$$

In the large N limit, diagrammatic contributions arrange in a topological expansion. At leading order, only disk diagrams contribute to the $2 \rightarrow 2$ pion amplitude.

$$\mathcal{T}_{ab}^{cd} = \underbrace{\text{Disk Diagram}}_{\sim 1/N} + \text{One-Loop Diagram} + \text{Two-Loop Diagram} + \dots$$

$\sim 1/N$ $\sim 1/N^2$ $\sim 1/N^3$

$\text{Tr}(T_a T_b T_d T_c) M(s, u)$ Flavor-ordered amplitude

Properties of $M(s,u)$

- **Crossing symmetry:** Invariance under the exchange of external pions implies

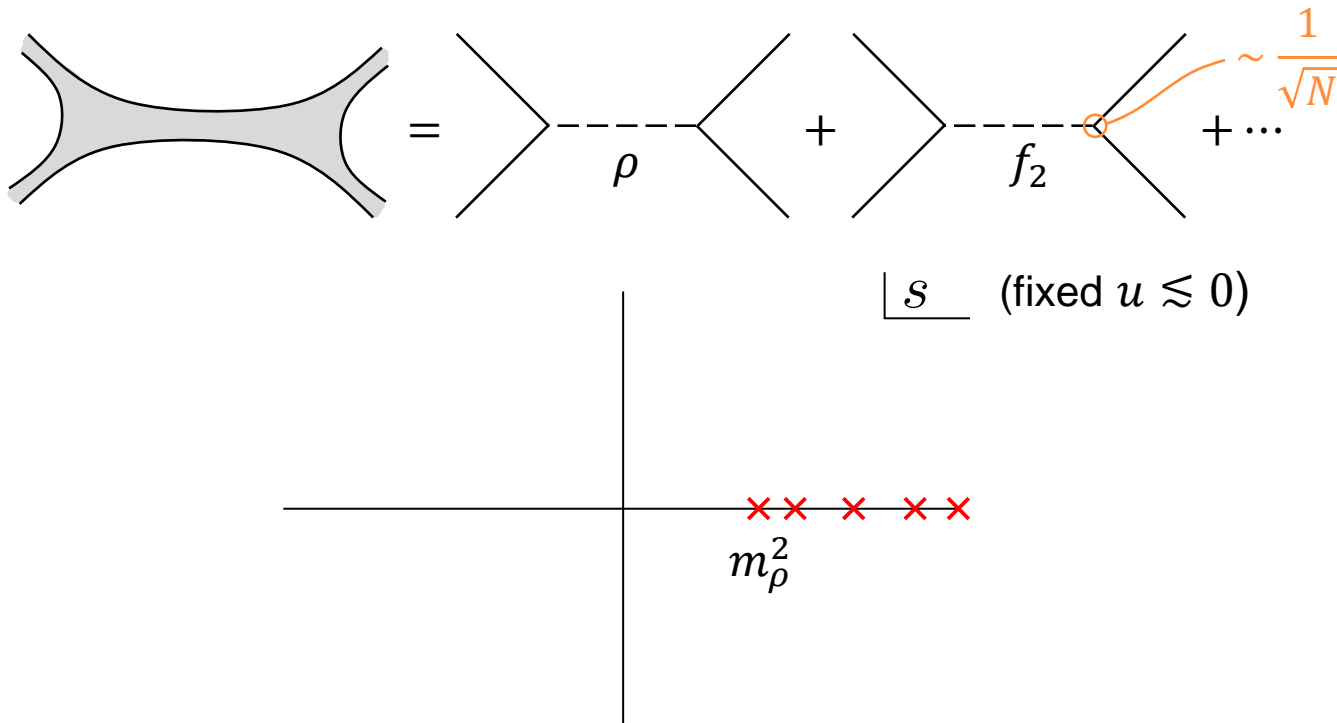
$$M(s, u) = M(u, s).$$

Properties of $M(s,u)$

- **Crossing symmetry:** Invariance under the exchange of external pions implies

$$M(s, u) = M(u, s).$$

- **Analytic structure:** $M(s, u)$ is **meromorphic** with poles from tree-level exchanges of physical mesons.



Properties of $M(s,u)$

- **Unitarity:** The residues of $M(s,u)$ admit a partial wave expansion with **positive** coefficients,

$$\text{Im } M(s,u) = \sum_{i \in \text{spect.}} \underbrace{\lambda_{\pi\pi i}^2 m_i^2}_{\geq 0} \pi \delta(s - m_i^2) P_{J_i} \left(1 + \frac{2u}{s} \right).$$

Properties of $M(s,u)$

- **Unitarity:** The residues of $M(s,u)$ admit a partial wave expansion with **positive** coefficients,

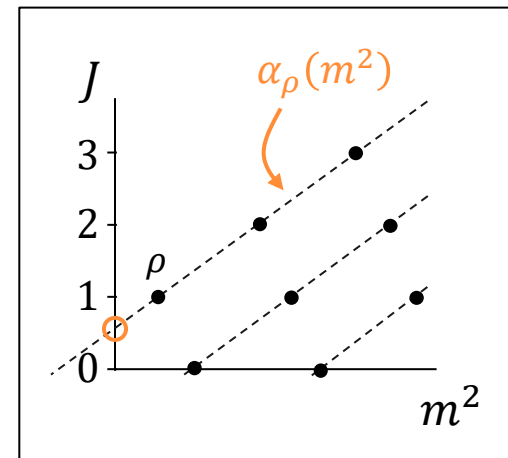
$$\text{Im } M(s,u) = \sum_{i \in \text{spect.}} \underbrace{\lambda_{\pi\pi i}^2 m_i^2}_{\geq 0} \pi \delta(s - m_i^2) P_{J_i} \left(1 + \frac{2u}{s} \right).$$

- **Regge behavior:** In the Regge limit of $|s| \rightarrow \infty$ with fixed $u \lesssim 0$, the growth of the amplitude is controlled by the intercept of the **leading Regge trajectory**,

$$M(s,u) \sim s^{\alpha(0)}.$$

This is the trajectory of the **rho**, so

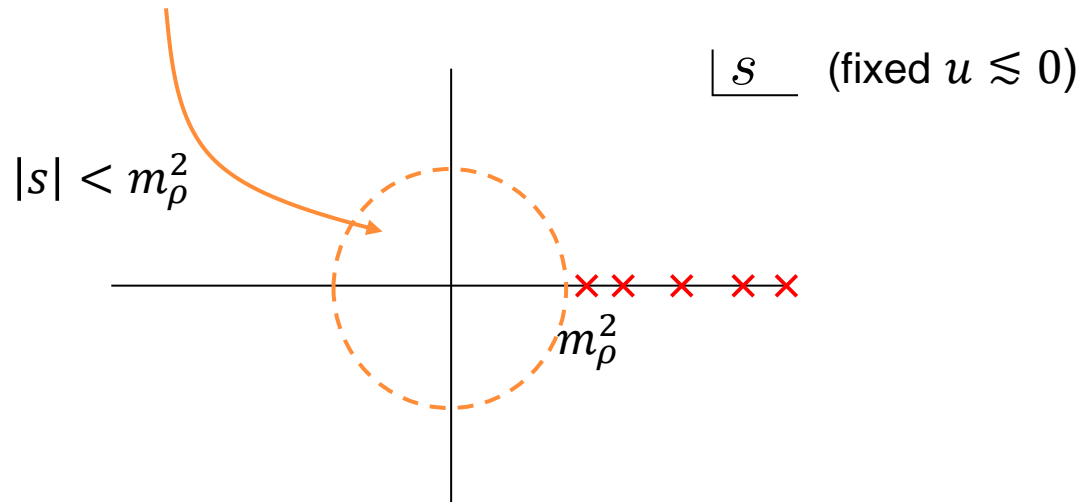
$$\lim_{|s| \rightarrow \infty} \frac{M(s,u)}{s} = 0.$$



Properties of $M(s,u)$

- **Low-energy expansion:** For energies below the first pole m_ρ^2 , $M(s,u)$ admits a **polynomial expansion**,

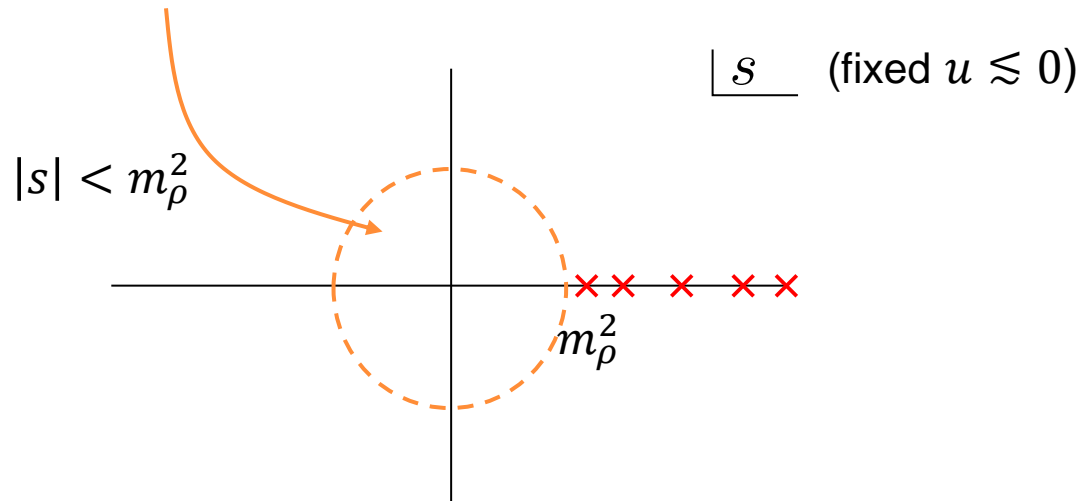
$$M_{\text{low}}(s,u) \approx g_{1,0}(s+u) + g_{2,0}(s^2+u^2) + 2g_{2,1}su + \dots$$



Properties of $M(s,u)$

- **Low-energy expansion:** For energies below the first pole m_ρ^2 , $M(s,u)$ admits a **polynomial expansion**,

$$M_{\text{low}}(s,u) \approx g_{1,0}(s+u) + g_{2,0}(s^2+u^2) + 2g_{2,1}su + \dots$$

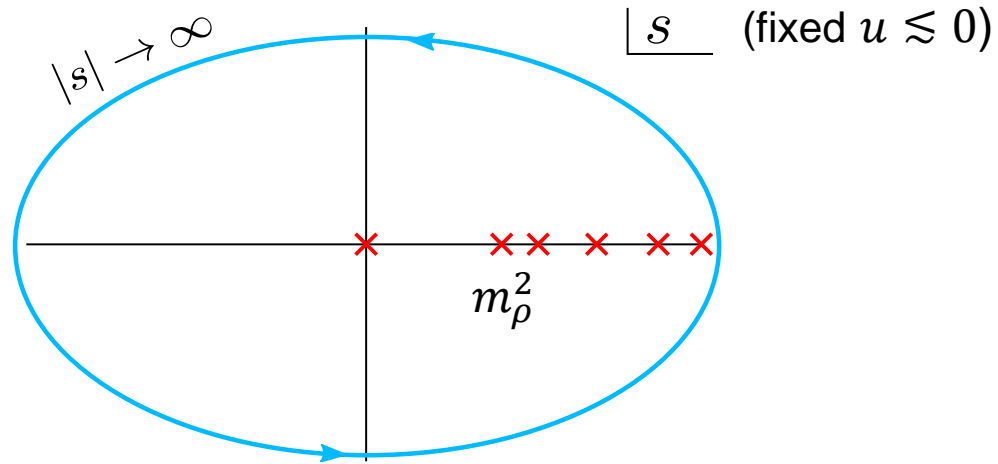


These coefficients are in one-to-one correspondence with Wilson coefficients of the **chiral Lagrangian**,

$$\mathcal{L}_{\text{Ch}} = -\frac{f_\pi^2}{4} \text{Tr}(\partial_\mu U^\dagger \partial^\mu U) + \kappa_1 \text{Tr}\left(\left(\partial_\mu U^\dagger \partial^\mu U\right)^2\right) + \kappa_2 \text{Tr}(\partial_\mu U^\dagger \partial_\nu U \partial^\mu U^\dagger \partial^\nu U) + \dots$$

Dispersion relations

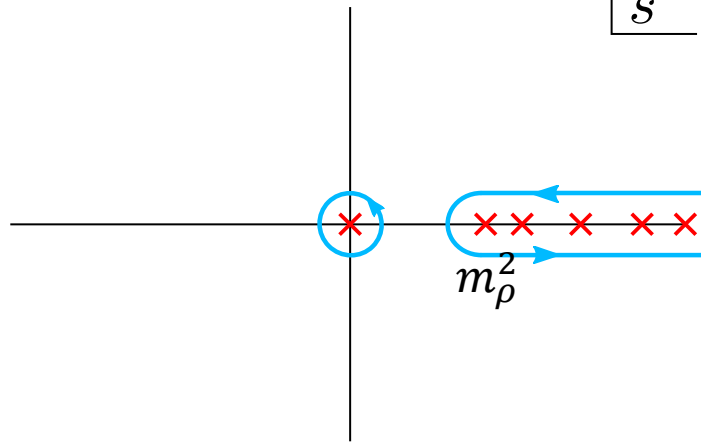
By the **Regge behavior**, $\frac{1}{2\pi i} \oint_{\infty} ds' \frac{M(s', u)}{s'^{k+1}} = 0. \quad (k = 1, 2, \dots)$



Dispersion relations

By the **Regge behavior**, $\frac{1}{2\pi i} \oint_{\infty} ds' \frac{M(s', u)}{s'^{k+1}} = 0. \quad (k = 1, 2, \dots)$

$|s|$ (fixed $u \lesssim 0$)

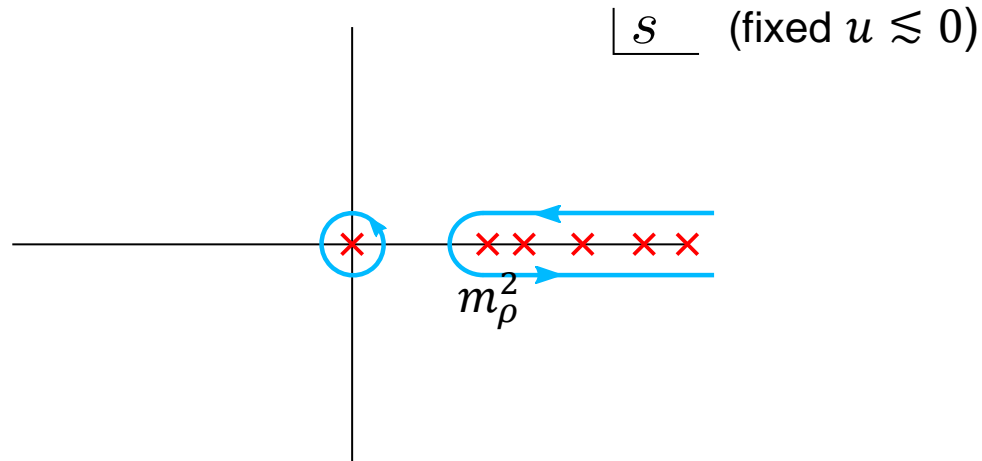


Deforming the contour yields a UV-IR link in the form of

Sum rules:
$$g_{n,\ell} = \sum_{i \in \text{spect.}} \underbrace{\lambda_{\pi\pi i}^2}_{\geq 0 \text{ (unitarity)}} F_{n,\ell}(J_i, m_i^2) \equiv \langle F_{n,\ell}(J, m^2) \rangle.$$

Dispersion relations

By the **Regge behavior**, $\frac{1}{2\pi i} \oint_{\infty} ds' \frac{M(s', u)}{s'^{k+1}} = 0$. ($k = 1, 2, \dots$)



Deforming the contour yields a UV-IR link in the form of

Sum rules: $g_{n,\ell} = \sum_{i \in \text{spect.}} \underbrace{\lambda_{\pi\pi i}^2}_{\geq 0 \text{ (unitarity)}} F_{n,\ell}(J_i, m_i^2) \equiv \langle F_{n,\ell}(J, m^2) \rangle.$

Crossing symmetry is encoded in an infinite set of

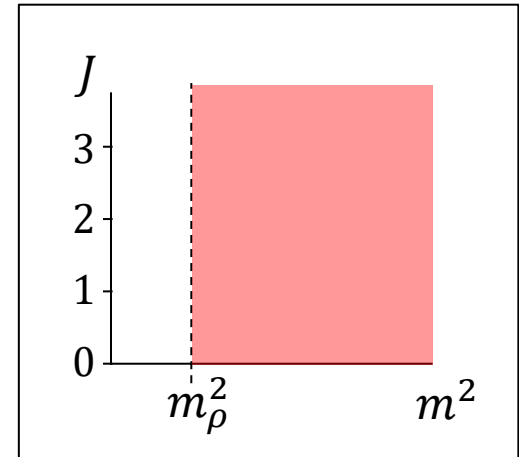
Null constraints: $0 = g_{n,\ell} - g_{n,n-\ell} = \langle \mathcal{N}_{n,\ell}(J, m^2) \rangle.$

Bootstrap bounds

We choose a potential **spectrum**, and we recast sum rules and null constraints into a **semidefinite program** to place bounds on:

- **Wilson coefficients:** When being agnostic about the heavy mesons, we can bound the effective pion couplings from integrating them out.

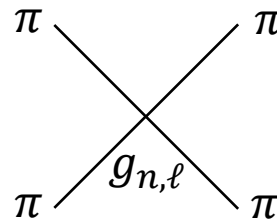
$$\begin{array}{ccc} \pi & & \pi \\ & \searrow & \nearrow \\ & g_{n,\ell} & \\ & \nearrow & \searrow \\ \pi & & \pi \end{array} \quad \longrightarrow \quad \frac{g_{n,\ell} m_\rho^{2(n-1)}}{g_{1,0}}$$



Bootstrap bounds

We choose a potential **spectrum**, and we recast sum rules and null constraints into a **semidefinite program** to place bounds on:

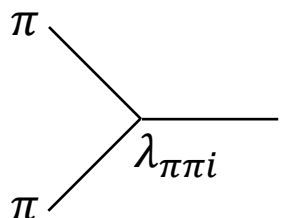
- **Wilson coefficients:** When being agnostic about the heavy mesons, we can bound the effective pion couplings from integrating them out.



A Feynman diagram showing two incoming pion lines (π) and two outgoing pion lines (π). The interaction is mediated by a vertex labeled $g_{n,\ell}$. An orange arrow points from the diagram to the following equation:

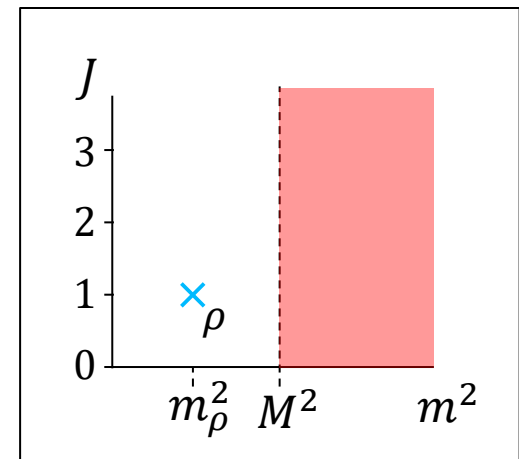
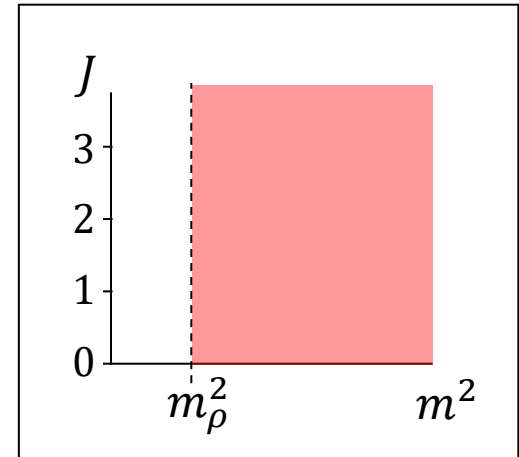
$$\frac{g_{n,\ell} m_\rho^{2(n-1)}}{g_{1,0}}$$

- **On-shell couplings:** If we refine our spectrum choice, we can directly probe their on-shell interactions.



A Feynman diagram showing two incoming pion lines (π) and one outgoing pion line (π) and one outgoing isospin line (i). The interaction is mediated by a vertex labeled $\lambda_{\pi\pi i}$. An orange arrow points from the diagram to the following equation:

$$\frac{\lambda_{\pi\pi i}^2}{g_{1,0} m_\rho^2}$$



Bounds on Wilson coefficients

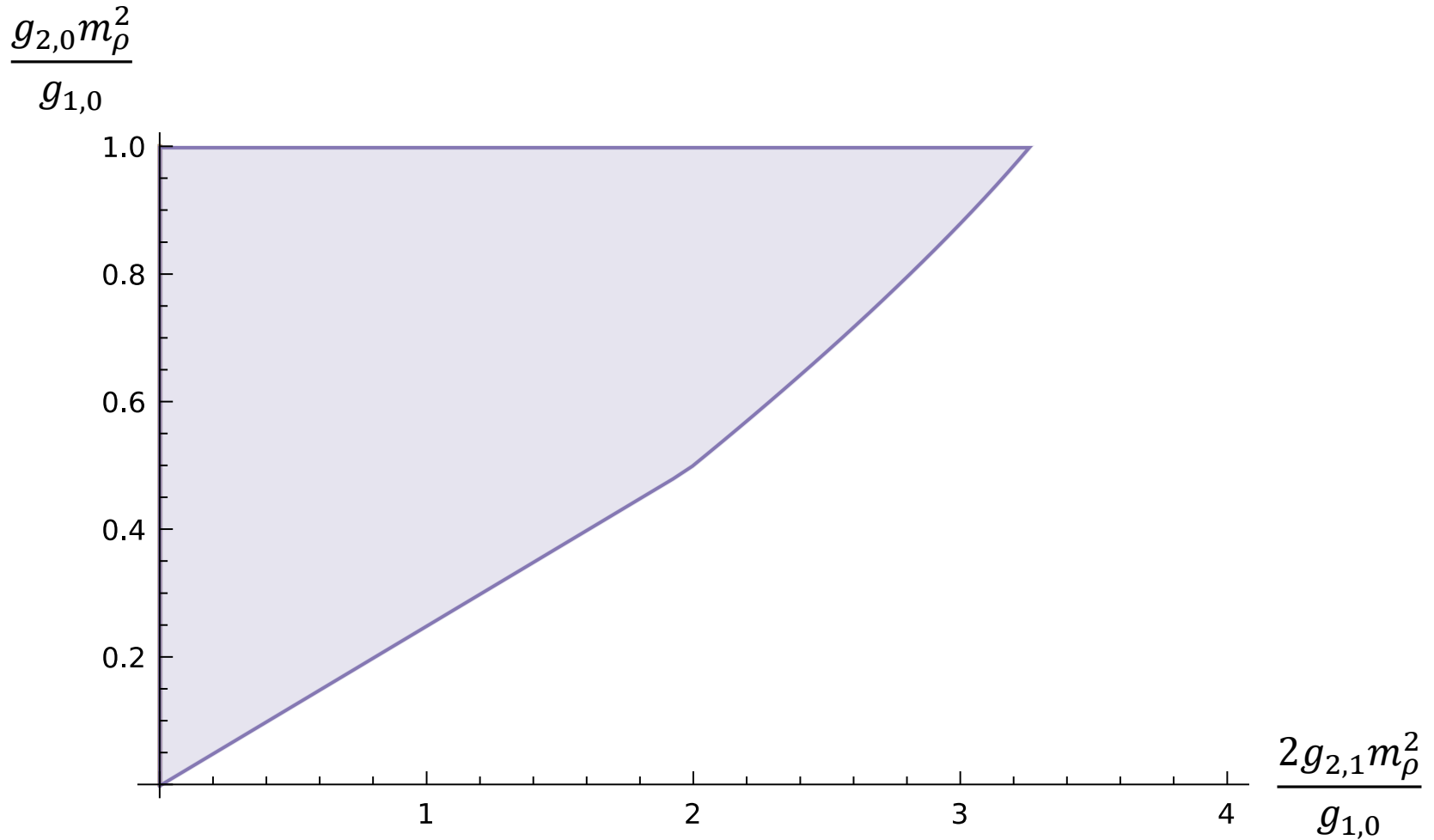


Figure 1: Allowed region in the space of (normalized) four-derivative couplings of the chiral Lagrangian.

Bounds on Wilson coefficients

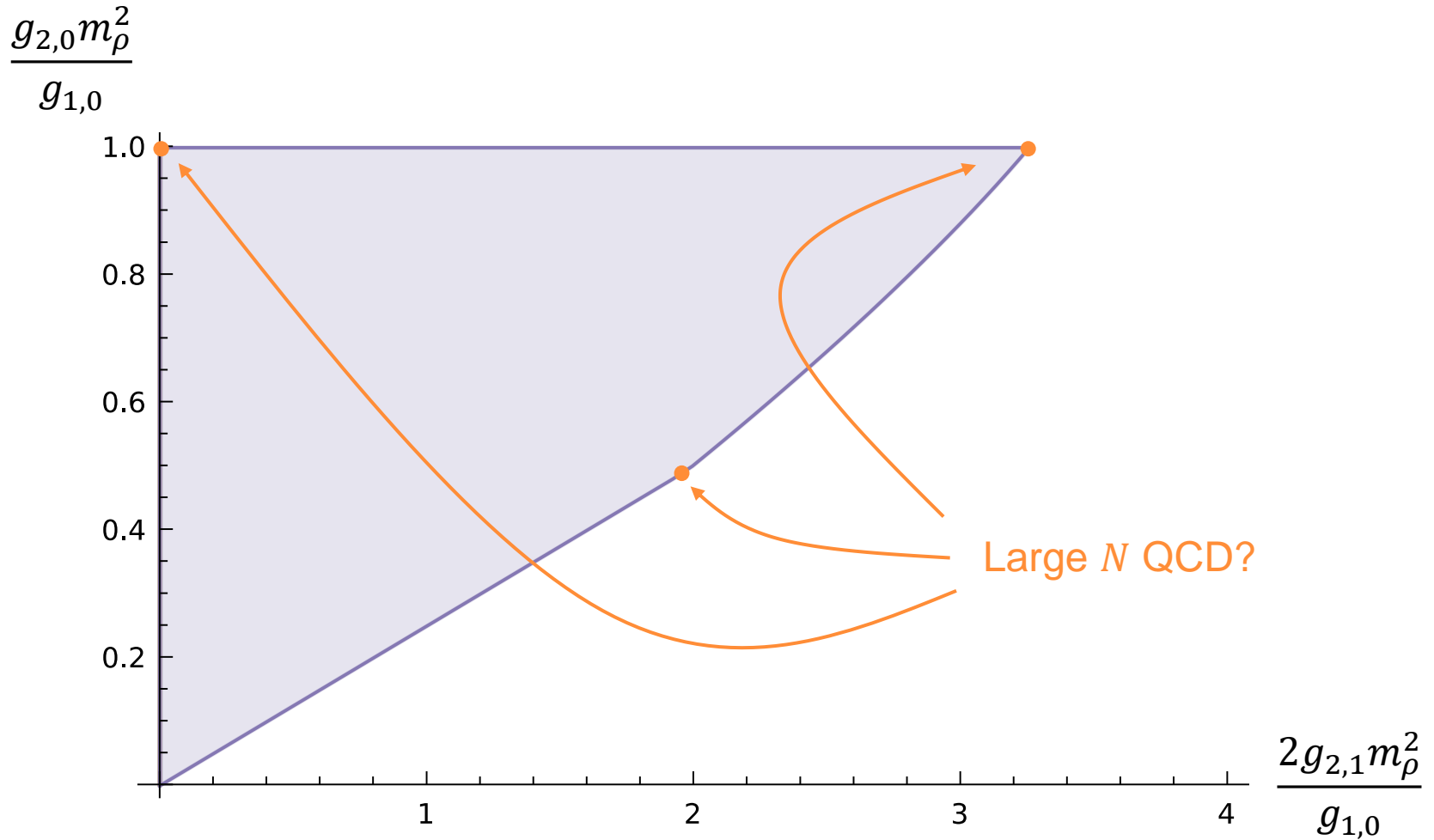


Figure 1: Allowed region in the space of (normalized) four-derivative couplings of the chiral Lagrangian.

Bounds on Wilson coefficients

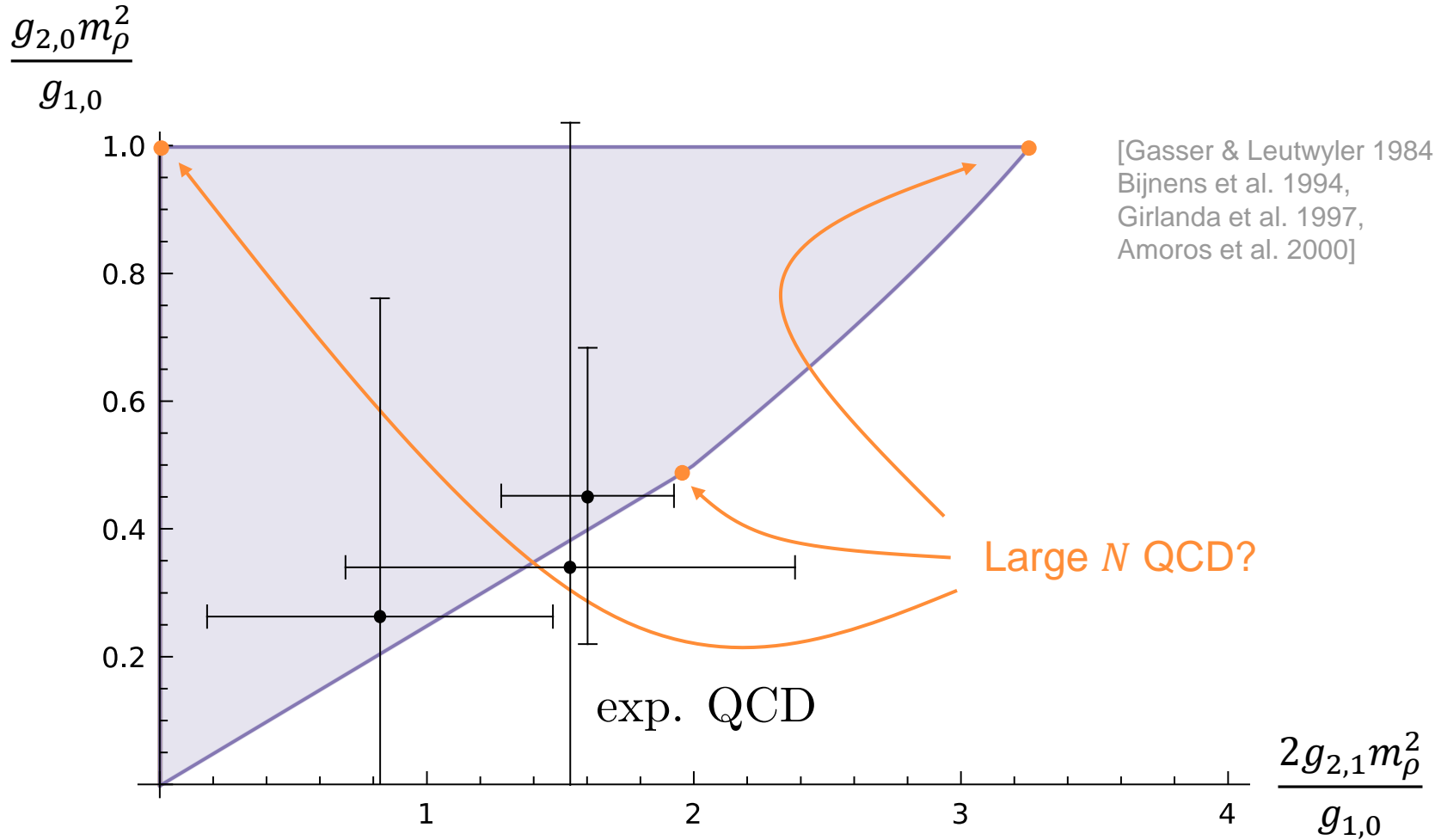


Figure 1: Allowed region in the space of (normalized) four-derivative couplings of the chiral Lagrangian.

Extremal amplitudes

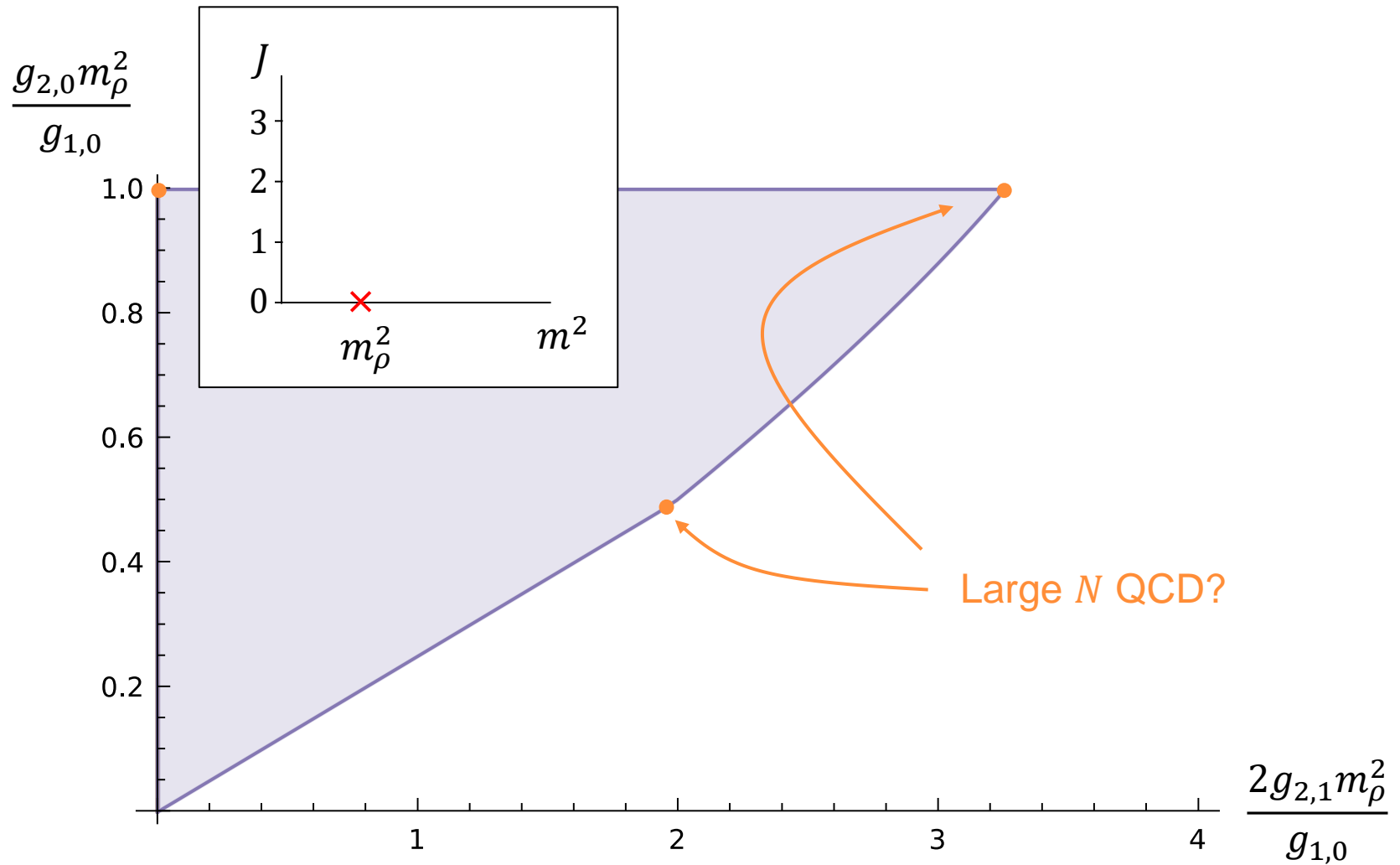


Figure 1: Allowed region in the space of (normalized) four-derivative couplings of the chiral Lagrangian.

Extremal amplitudes

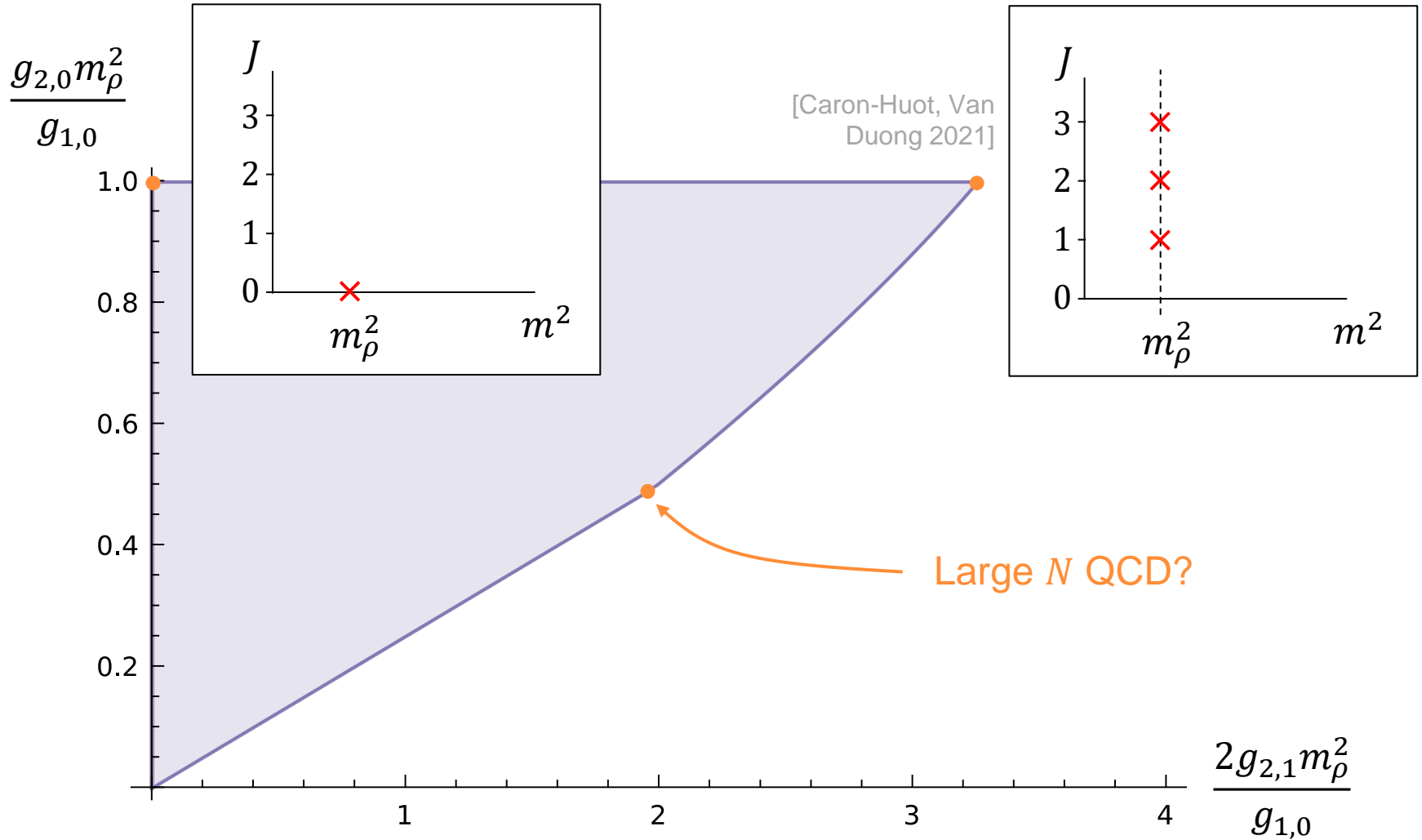


Figure 1: Allowed region in the space of (normalized) four-derivative couplings of the chiral Lagrangian.

Extremal amplitudes

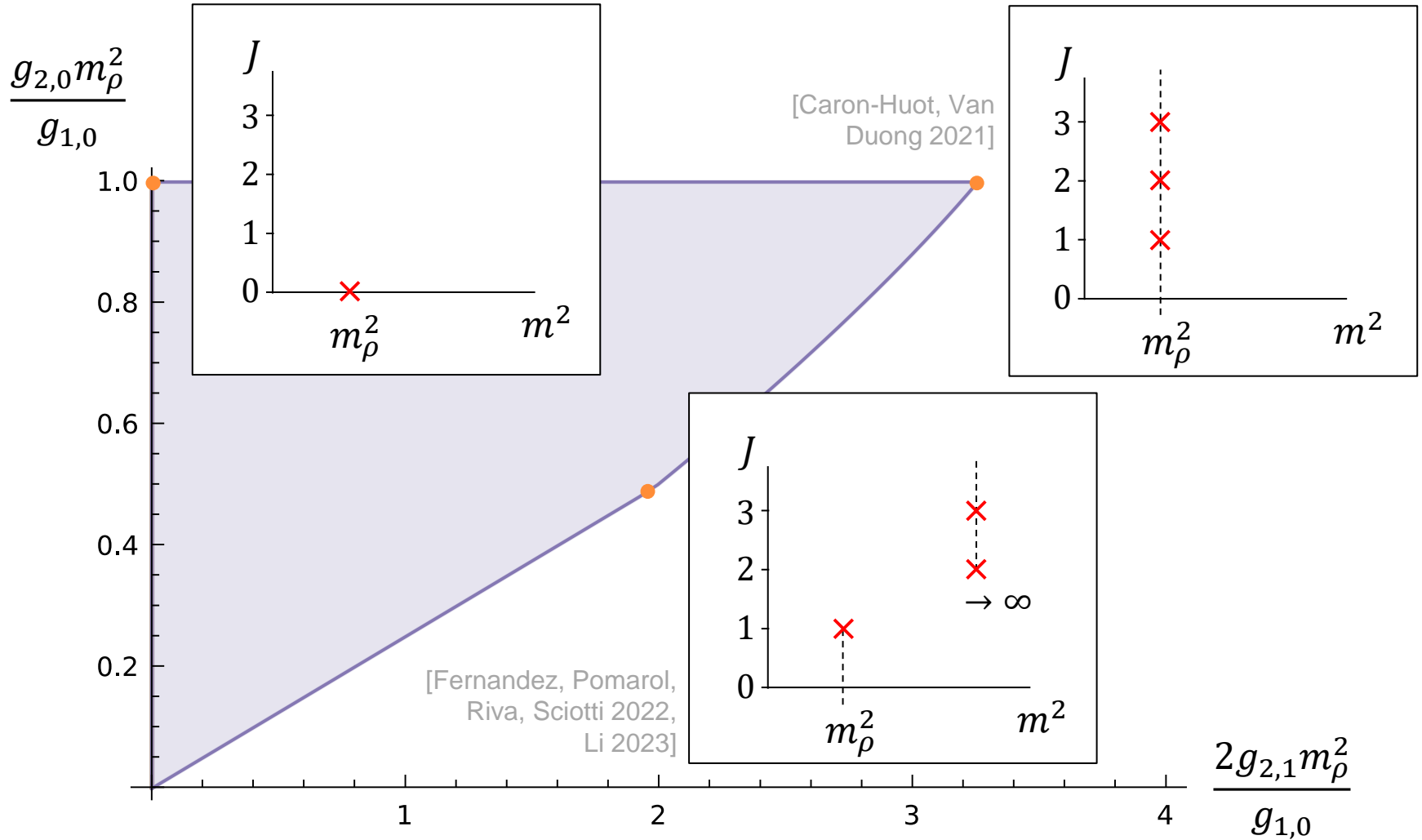
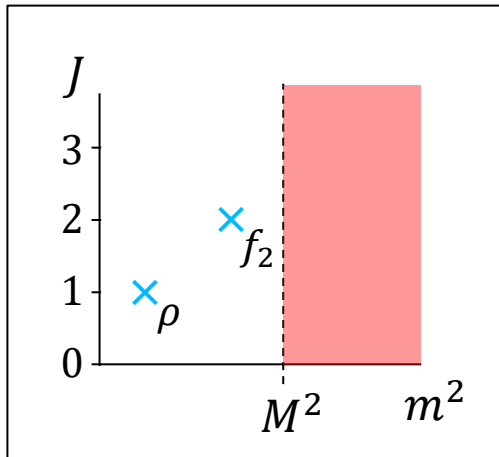


Figure 1: Allowed region in the space of (normalized) four-derivative couplings of the chiral Lagrangian.

Bounds on on-shell couplings



Bounds on on-shell couplings

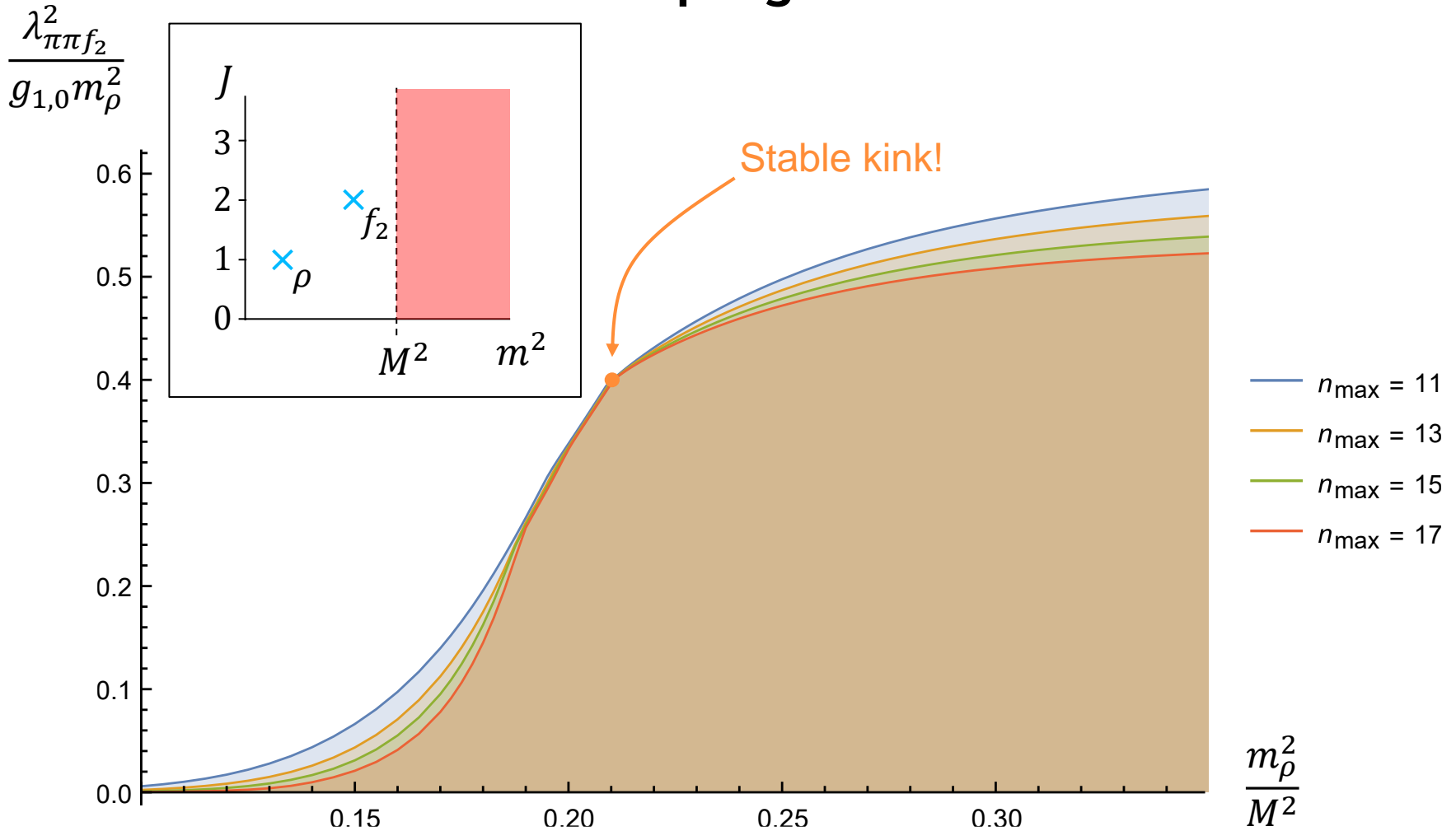


Figure 2: Upper bound on the (normalized) f_2 on-shell coupling as a function of the gap after the f_2 .

Bounds on on-shell couplings

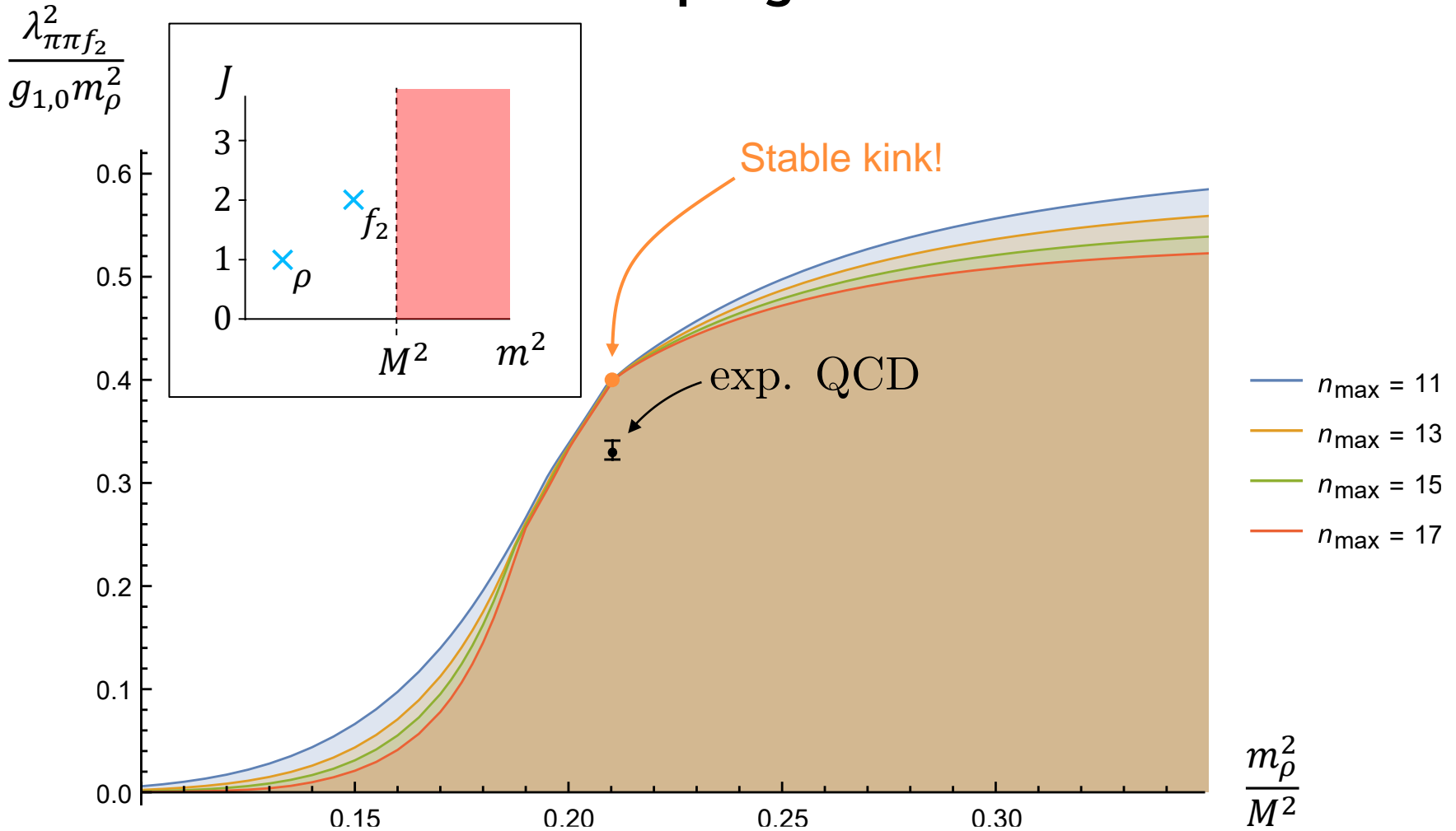


Figure 2: Upper bound on the (normalized) f_2 on-shell coupling as a function of the gap after the f_2 .

Ratio of couplings

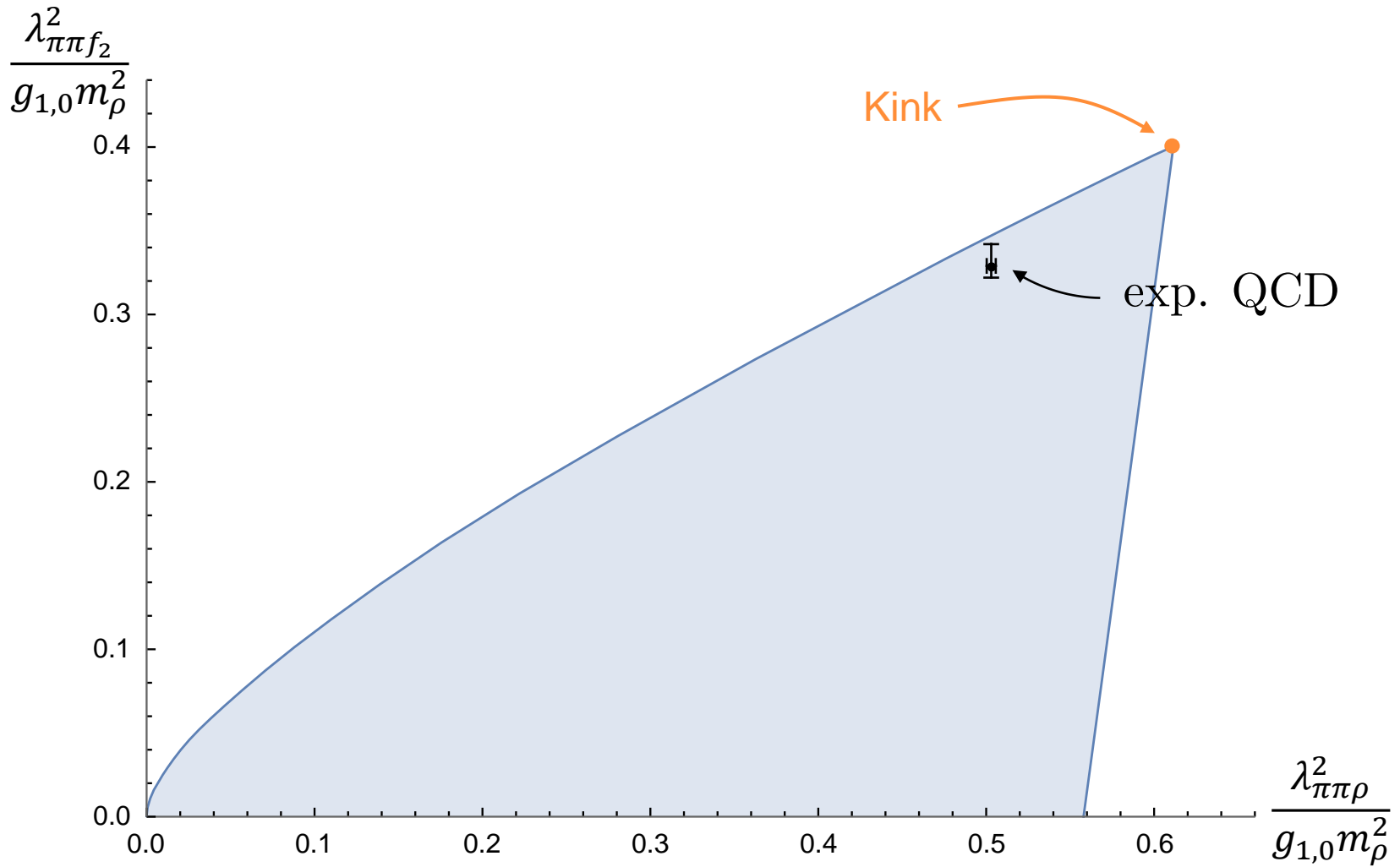


Figure 3: Exclusion plot in the space of (normalized) on-shell couplings for the rho and the f_2 .

Ratio of couplings

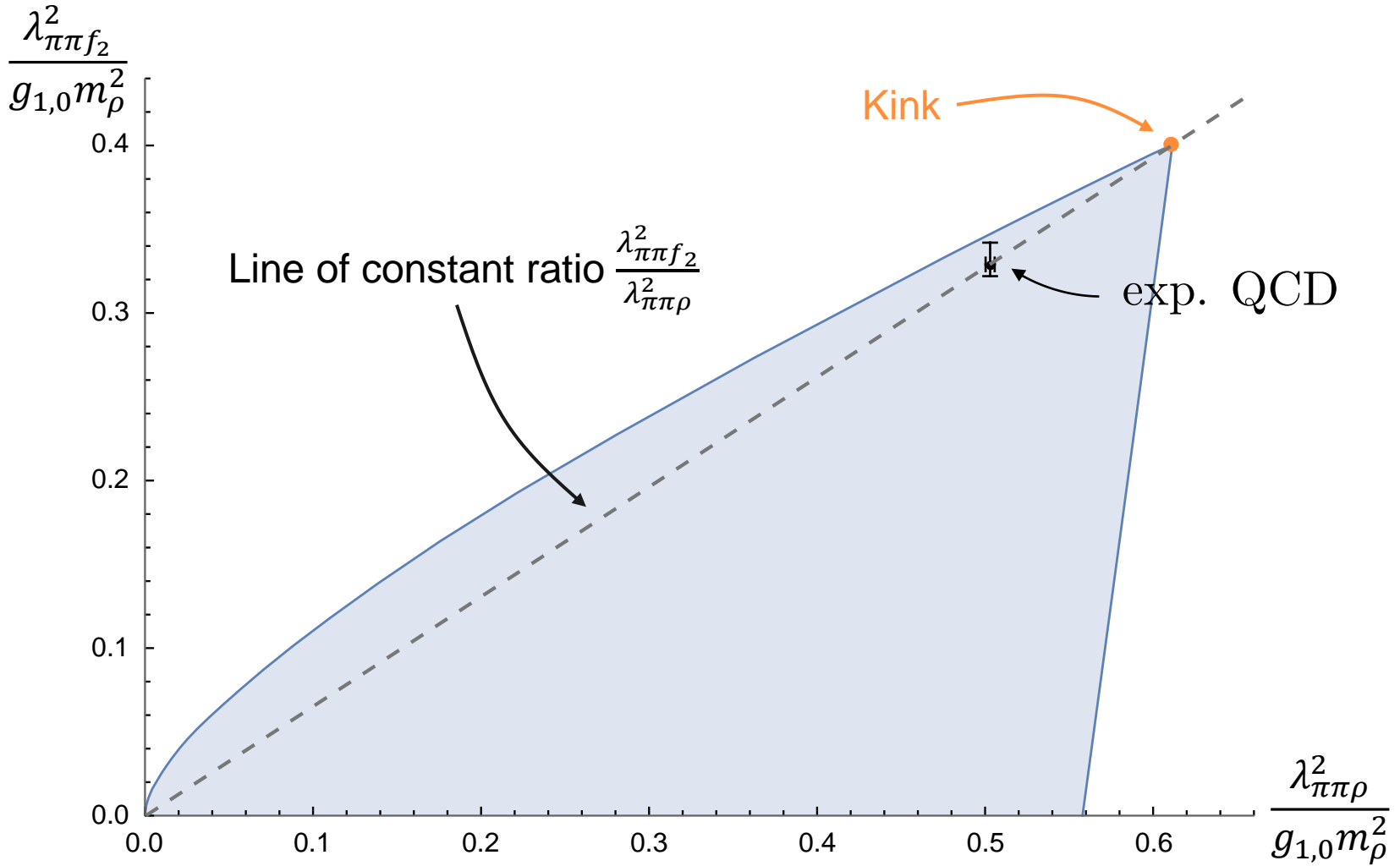


Figure 3: Exclusion plot in the space of (normalized) on-shell couplings for the rho and the f_2 .

Spectrum at the kink

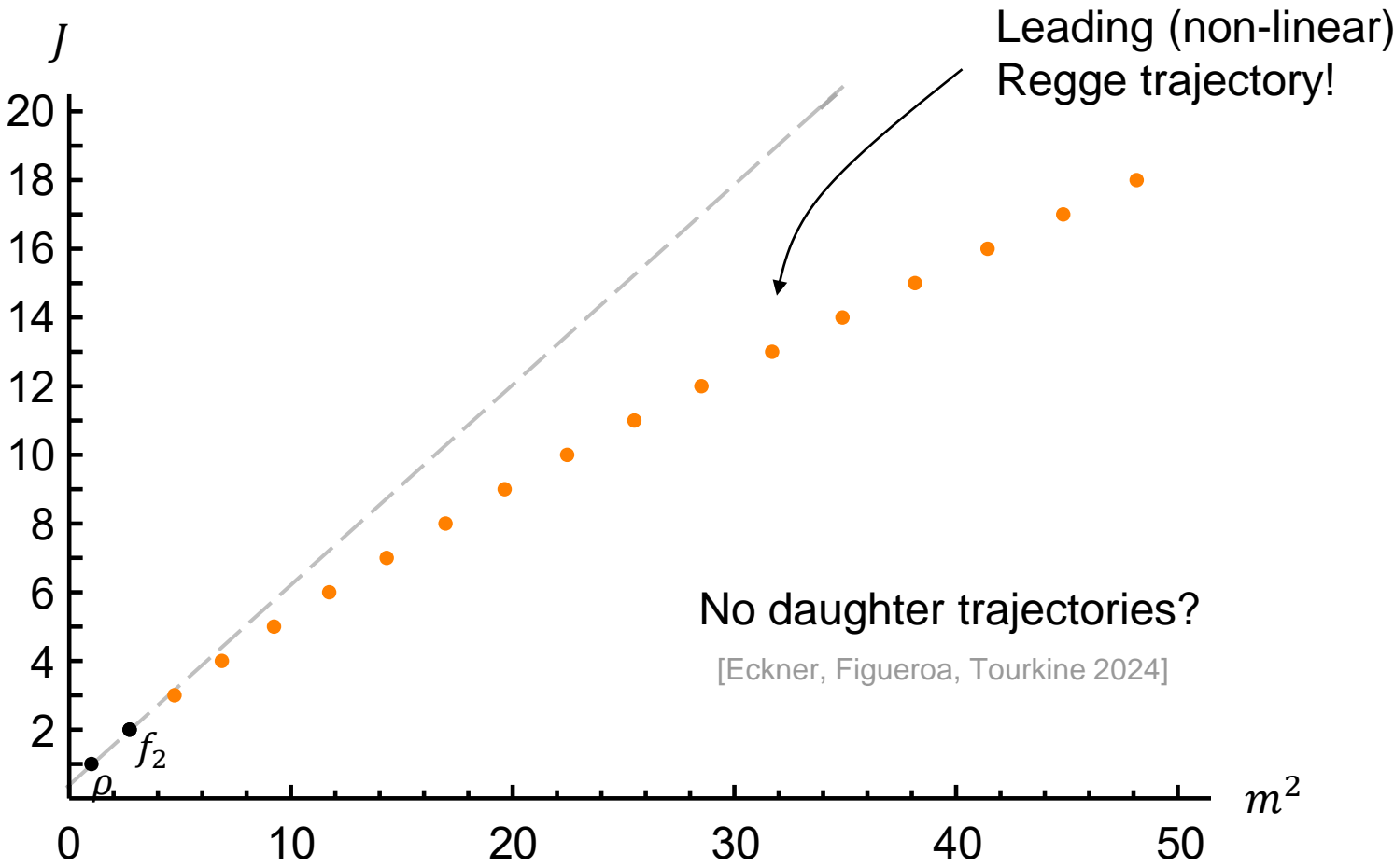


Figure 4: Spectrum of the numerical solution at the kink.

Spectrum of QCD

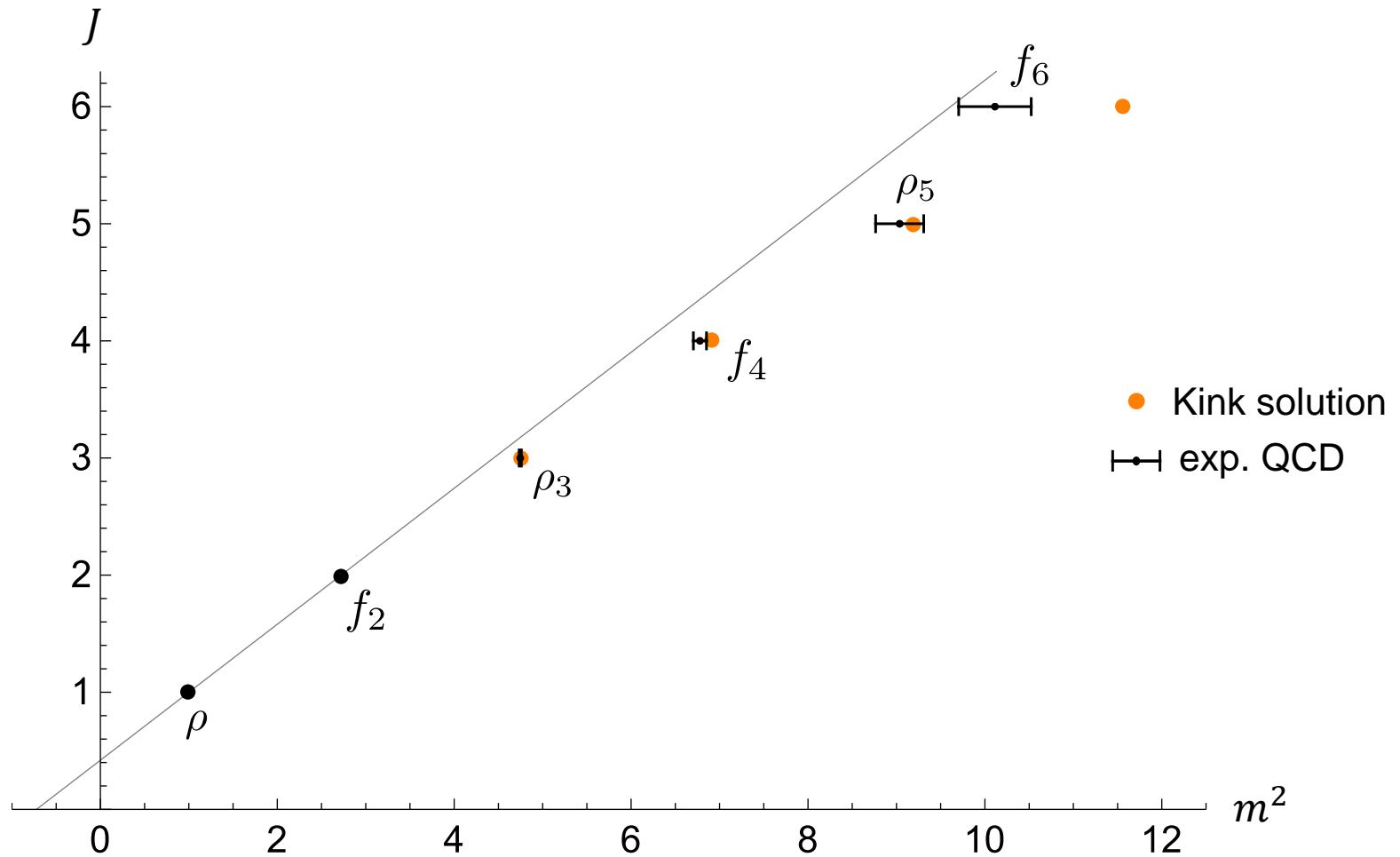
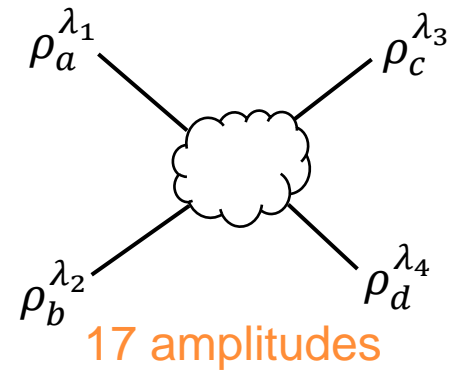
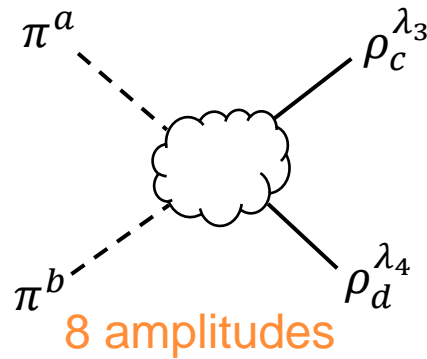
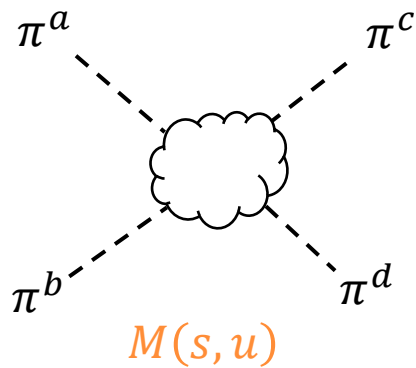


Figure 5: Comparison of the spectra of the extremal solution and real-world QCD.

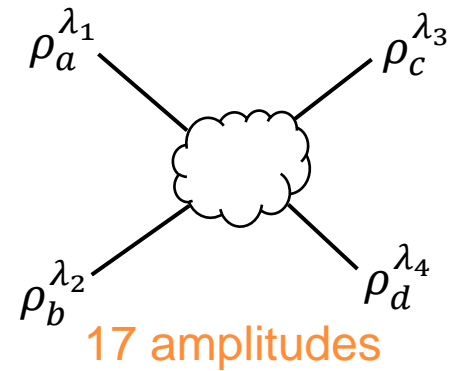
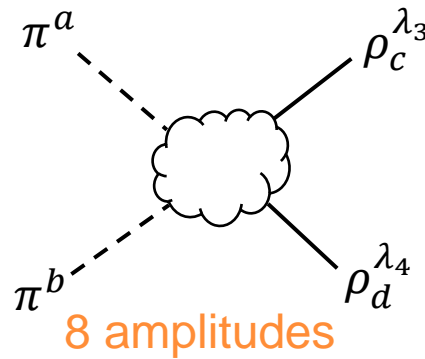
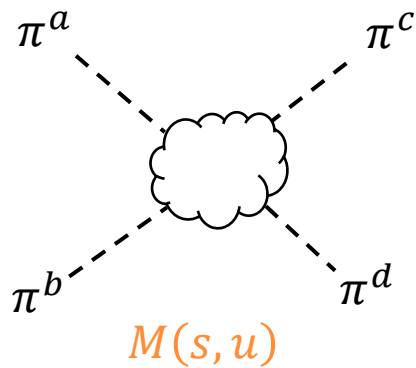
Mixed S-matrices

Many more constraints come from considering a mixed scattering system of **pions and rho mesons**. But the difficulty grows quickly with spin.



Mixed S-matrices

Many more constraints come from considering a mixed scattering system of **pions and rho mesons**. But the difficulty grows quickly with spin.



A simpler system is that of **pions and photons**, which captures the **chiral anomaly**. Matching the anomaly yields bounds with an explicit dependence on N/f_π^2 .

$$J_A^a \times \text{triangle} = \pi^0 \text{---} \gamma \propto \frac{e^2 N}{16\pi^2 f_\pi} \pi^0 F \wedge F$$

Conclusions

Summary:

- We are **carving out** the space of large N confining gauge theories.
- Generic bounds on **Wilson coefficients** are saturated by simple solutions.
- The key seems to be to include explicit poles up to **spin two**.
- This reveals a kink with many features in common with **real-world QCD**.

“Have we cornered large N QCD?”

Not clear yet, but we’re getting tantalizingly close.”

Conclusions

Summary:

- We are **carving out** the space of large N confining gauge theories.
- Generic bounds on **Wilson coefficients** are saturated by simple solutions.
- The key seems to be to include explicit poles up to **spin two**.
- This reveals a kink with many features in common with **real-world QCD**.

“Have we cornered large N QCD?”

Not clear yet, but we’re getting tantalizingly close.”

Future directions:

- Include external rho mesons. [in progress: JA, Henriksson, Rastelli, Vichi]
- Consider general background gauge fields and anomalies.
- Explore the glueball and baryon sectors.
- Target other weakly coupled systems.

(e.g. tree-level string theory. [to appear: JA, Knop, Rastelli])

- Etc!

Thank you!

